

CONVEX OPTIMIZATION-BASED EMERGENCY LANDING TRAJECTORY GENERATION FOR UAM VEHICLES

Yeondeuk Jung[1], Sungwook Cho[2]
[1]Korea Aerospace Research Institute
[2]Cheongju University

Abstract

Urban Air Mobility (UAM) and Advanced Air Mobility (AAM) require electric vertical takeoff and landing (eVTOL) aircraft to maintain safe landing capability under contingency conditions. In particular, when a propulsion-system anomaly occurs, the aircraft must generate a controlled emergency-landing trajectory from its current state while satisfying thrust, landing-geometry, and terminal-descent constraints. This paper presents a regulation-informed convex trajectory-generation framework for eVTOL emergency landing. The framework uses representative controlled-emergency-landing requirements from the European Union Aviation Safety Agency (EASA) and the Federal Aviation Administration (FAA) as design references to define a two-phase landing profile composed of a landing-approach phase and a terminal-descent phase. The non-convex thrust-magnitude constraint is handled using lossless convexification, and the resulting problem is formulated as a second-order cone program. A numerical example shows that the generated trajectory satisfies the thrust and landing-geometry constraints. The relaxation gap and lower-thrust margin further provide numerical evidence of feasibility for the tested scenario.

Keywords: Urban Air Mobility, Emergency Landing, Trajectory Generation, Convex Optimization, Lossless Convexification

1. Introduction

As Urban Air Mobility (UAM) and Advanced Air Mobility (AAM) continue to develop, emergency-landing capability has become a key safety requirement for electric vertical takeoff and landing (eVTOL) aircraft. In particular, in contingency situations such as a propulsion-system anomaly, the aircraft must be able to perform a controlled emergency landing (CEL). This capability is a core safety design objective commonly identified in EASA's SC-VTOL and in representative FAA powered-lift special-class airworthiness criteria. Unlike the glide of fixed-wing aircraft or the autorotation of rotorcraft, an eVTOL has limited passive means for emergency landing, so an emergency-landing trajectory must be generated through active thrust control.

Because a contingency demands an immediate response, the emergency-landing trajectory must be generated in real time onboard the aircraft from its current state, rather than relying on a ground control station. At the same time, the generated trajectory must satisfy a number of constraints, including thrust magnitude and direction limits, the landing geometry, and safe-descent conditions. However, when a non-convex constraint such as a lower bound on the thrust magnitude is present, the trajectory-generation problem becomes a non-convex optimization problem, for which it is difficult to guarantee both real-time performance and global optimality.

Convex-optimization-based trajectory generation has attracted attention as an approach to overcome this difficulty. In particular, in the field of powered-descent guidance for planetary landing, the lossless convexification (LCvx) technique, which transforms a non-convex constraint into an equivalent convex problem, has been proposed, and its real-time performance and global convergence have been established [1]. Such convex-optimization-based approaches have been demonstrated in onboard real-time implementations [2], and more recently their application to descent and landing trajectory generation for UAM/eVTOL has been expanding [3], [4]. This trend motivates the application of a convex-optimization-based approach to eVTOL

emergency-landing trajectory generation.

This paper presents a regulation-informed convex trajectory-generation framework for eVTOL emergency landing and demonstrates its feasibility through simulation. The framework defines a two-phase landing profile, consisting of a landing-approach phase and a terminal-descent phase, using representative CEL requirements from EASA and FAA as design references, and it formulates the resulting problem as a second-order cone program through LCvx. The remainder of this paper is organized as follows. Section 2 defines the emergency-landing problem operationally and with respect to the regulations; Section 3 describes the convex trajectory-generation framework; Section 4 presents the simulation results; and Section 5 concludes the paper.

2. Operational Problem Definition

2.1 Target vehicle and landing mode

The target vehicle of this study is the Optionally Piloted Personal Air Vehicle (OPPAV) developed by the Korea Aerospace Research Institute (KARI), whose configuration is shown in Figure 2. The vehicle has eight propellers, arranged with four forward and four aft of the main wing. It is a single-seat vehicle with a length of approximately 6.2 m, a wingspan of approximately 7 m, and a maximum takeoff weight of approximately 680 kg.

This paper considers emergency landing in a hover-capable vertical flight mode. Although the OPPAV has a main wing, emergency touchdown at a confined urban landing site requires vertical-flight landing capability rather than forward-flight or transition-mode operation. Therefore, this study focuses on emergency landing in the vertical flight mode; forward-flight and transition dynamics are outside its scope. Because immediate pilot intervention cannot be assumed during a contingency, autonomous emergency landing is considered.

The emergency-landing trajectory generation is based on a three-degree-of-freedom (3-DoF) point-mass model describing the translational motion of the aircraft. In the vertical flight mode, the attitude dynamics are sufficiently fast relative to the translational dynamics, so it is reasonable to treat the attitude and translational dynamics separately. Accordingly, the framework treats thrust magnitude and direction as guidance-level control inputs and generates a translational reference trajectory using the point-mass model. Extension to six-degree-of-freedom (6-DoF) dynamics that include attitude as a state variable is left for future work. Nevertheless, to indirectly reflect attitude constraints, a constraint on the direction (tilt) of the thrust vector is considered. The generated trajectory serves as a translational guidance reference to be tracked by a lower-level attitude-control and thrust-allocation controller, and closed-loop 6-DoF flight-dynamics verification is outside the scope of this paper.

2.2 Contingency landing as the operational setting

This paper considers a contingency in which a propulsion-system anomaly, such as a failure, prevents the aircraft from reaching its originally intended destination (e.g., a vertiport). In such a situation, the aircraft must immediately perform a controlled emergency landing (CEL) and touch down safely at an emergency landing site that has been designated in advance or identified during flight. Because a contingency demands an immediate response, the emergency-landing trajectory must be generated in real time from the current state of the aircraft. Accordingly, this paper aims to generate a descent trajectory that takes as input the aircraft state at the onset of the contingency and the coordinates of the designated emergency landing site, and that satisfies the vehicle's motion limits and the constraints for a safe landing.

CEL is a design requirement commonly prescribed in the airworthiness criteria of EASA and the FAA. EASA defines CEL in VTOL.2000(b)(4) of the Special Condition for small-category VTOL aircraft (SC-VTOL-01, Issue 1, 2019) [5], specifying it as a landing in which the aircraft can perform a controlled landing, can use emergency procedures if necessary, does not require exceptional piloting skill or strength, and in which some damage to the aircraft is acceptable. Furthermore, EASA's Means of Compliance (MOC) allows autorotation to be replaced by CEL when referring to existing rotorcraft regulations, thereby shifting from a prescriptive criterion that directly required autorotation capability to a performance-based criterion that requires a controlled-emergency-landing capability [6].

The FAA type-certifies powered-lift eVTOLs as special-class aircraft under 14 CFR 21.17(b). In representative criteria such as the Special Class Airworthiness Criteria for the Joby Model JAS4-1 (2024), CEL is defined in JS4.2000. JS4.2105(g) further requires the aircraft to be capable of performing a CEL after loss of power or

thrust, by glide, autorotation, or an equivalent means [9]. The performance level of CEL intended by the FAA is to provide equivalence to the glide requirement for fixed-wing aircraft (14 CFR Part 23) and the autorotation requirement for rotorcraft (14 CFR Part 27).

Since the target vehicle of this paper is also a powered-lift eVTOL that lands in the vertical flight mode, this study identifies, among these regulations, the requirements applicable to emergency landing in the vertical flight mode and reflects them in the design of the emergency-landing profile. This paper does not, however, aim to demonstrate certification compliance with any specific airworthiness criterion; the regulations are used as design references to define the emergency-landing profile and the terminal conditions.

2.3 Regulation-informed landing geometry

Rotorcraft airworthiness criteria (CS-27 and 14 CFR Part 27) do not prescribe a single touchdown sink-rate limit applicable to all aircraft. Instead, they require the landing-gear shock-absorption capability to be substantiated through ground-load assumptions (Sec. 27.473) and through the limit and reserve-energy drop tests (Sec. 27.725, Sec. 27.727) used to verify this capability [8]. With reference to these, this study interprets the touchdown sink rate allowable for a given vehicle's landing-gear design as a terminal boundary condition of the terminal-descent phase. This condition is expressed in the framework as a velocity-type terminal constraint, but its actual limiting value is determined by the landing-gear design and test criteria of the target vehicle.

The transition point from the landing-approach phase to the terminal phase is defined as the junction. The identification of this transition point adopts the Landing Decision Point (LDP) identification criterion prescribed in VTOL.2130(c) of EASA MOC-2 SC-VTOL [6], namely the identification by a combination of height, vertical speed, and airspeed and/or ground speed. However, since the definition of the LDP is based on the possibility of a balked landing, whereas a CEL does not assume a balked landing, that definition cannot be applied directly. Accordingly, this study does not treat the transition point as an LDP in the regulatory sense. Instead, it is defined as a kinematic transition point at which a safe landing through stabilized terminal descent should begin. This point is referred to as the terminal landing-phase junction, and only the LDP identification concept is adopted. Moreover, since no specific regulatory value exists for the junction altitude, this study adopts, as a representative design reference, the height (h2 = 30.5 m, 100 ft) of Reference Volume Type 1 given in the non-binding EASA PTS-VPT-DSN guidance for vertiport design [7] as the junction altitude.

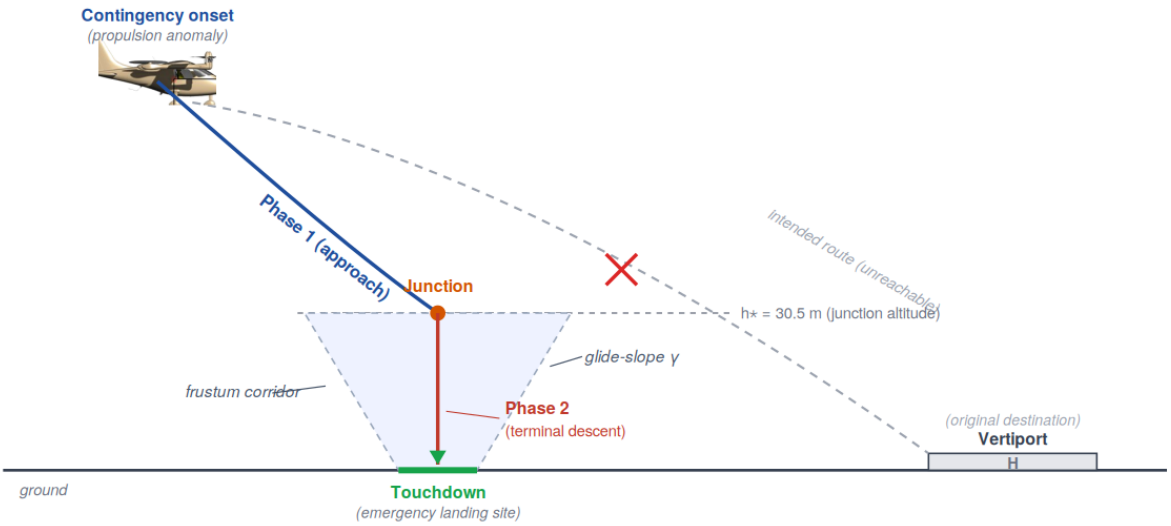


Figure 1 – Operational scenario and landing geometry for emergency landing.

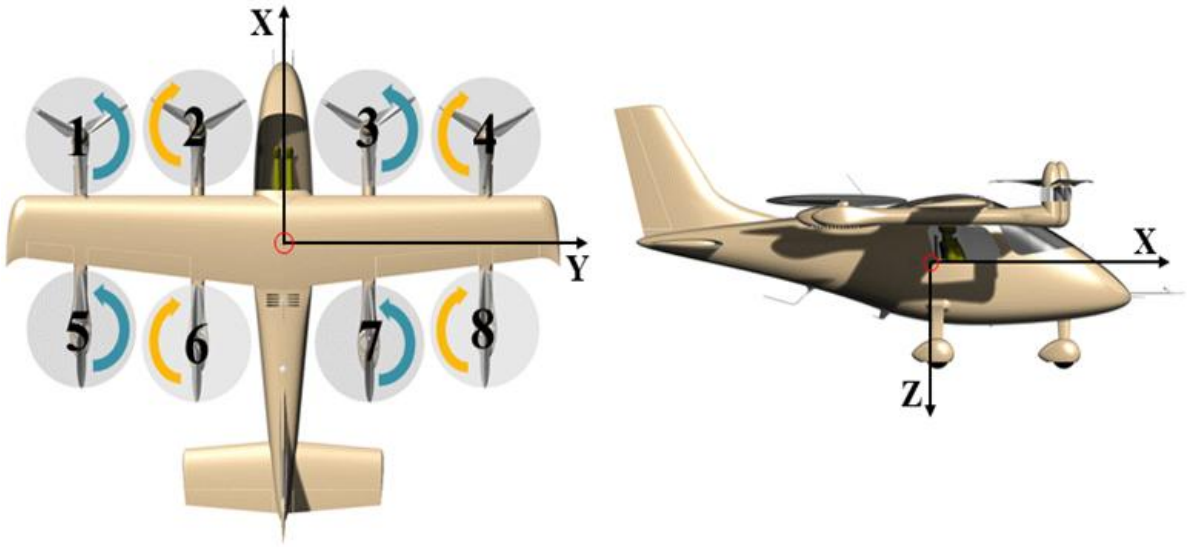


Figure 2 – eVTOL-based UAM vehicle (OPPAV) configuration.

3. Convex Trajectory-Generation Framework

3.1 Problem setup and dynamics

This section describes the convex-optimization-based trajectory-generation framework for the emergency-landing problem defined in Section 2. The problem is to generate, in real time, a landing trajectory from the aircraft state at contingency onset to the designated emergency landing site, while satisfying the vehicle's maneuver limits and the constraints for a safe landing. The inputs are the aircraft state at contingency onset, the coordinates of the designated emergency landing site, and the vehicle's maneuver limits; the output is a landing trajectory that satisfies the terminal boundary conditions. The trajectory is generated with a two-phase structure consisting of a landing-approach phase and a terminal-descent phase, and the two phases are connected at the terminal landing-phase junction defined in Section 2.3.

The translational motion of the aircraft is described by a 3-DoF point-mass model. The state x = (p, v) consists of the position p and velocity v in the inertial frame, and the control input u is the thrust vector. The translational dynamics are given by

$$\dot{p}(t) = v(t), \qquad \dot{v}(t) = \frac{1}{m}\,u(t) + g \tag{1}$$

where m is the vehicle mass, g is the gravitational acceleration vector, and e3 is the inertial upward unit vector. In matrix form, the dynamics are written as

$$\dot{x}(t) = A\,x(t) + B\,u(t) + c, \quad A = \begin{bmatrix} 0_3 & I_3 \\ 0_3 & 0_3 \end{bmatrix}, \quad B = \begin{bmatrix} 0_3 \\ \frac{1}{m} I_3 \end{bmatrix}, \quad c = \begin{bmatrix} 0_3 \\ g \end{bmatrix} \tag{2}$$

which is a linear time-invariant (LTI) system with a constant drift.

3.2 Constraints

Constraints are imposed on both the magnitude and the direction of the thrust. First, the thrust magnitude has the following annular bounds, determined by the available range of the propulsion system:

$$u_{\min} \le \|u(t)\| \le u_{\max} \tag{3}$$

where the lower bound u_min > 0 is the minimum thrust and the upper bound u_max is the maximum thrust. The non-convexity due to this lower bound is the only source of non-convexity in the problem. The direction of the thrust vector is restricted by the following tilt-cone constraint:

$$\|H_c\,u(t)\| \le \tan(\theta_{\max})\,e_3^{\top} u(t) \tag{4}$$

where Hc is the projection onto the horizontal components and theta_max is the maximum tilt half-angle from the inertial upward direction. This constraint restricts the thrust direction to within theta_max of the vertical axis

and, as described in Section 2.1, indirectly reflects attitude constraints in the point-mass model. Since the right-hand side must be non-negative, an upward thrust component is automatically implied.

The constraints on the landing geometry correspond to the emergency-landing profile described in Section 2.3. In the terminal-descent phase, the aircraft descends along the interior of a frustum corridor with the landing site at its apex, which is expressed by the following glide-slope constraint:

$$\|H_c\, p(t) - c_{td}\| \le R_{td} + \cot(\gamma_{\text{glide}})\left(e_3^\top p(t) - h_{td}\right) \tag{5}$$

where c_td and h_td are the horizontal position and the altitude of the landing site, R_td is the landing-disk radius, and gamma_glide is the glide-slope angle. In addition, the altitude of the aircraft is restricted by an altitude box, and ascent is prohibited in the terminal-descent phase:

$$0 \le e_3^\top p(t) - h_{td} \le h_{\text{top}} \tag{6}$$

In emergency landing, the touchdown sink rate must be limited to within the landing-gear design limit of the target vehicle. In this paper, the safe-descent condition is reflected in a limited manner through the terminal sink-rate boundary condition and the landing-geometry constraints, while the derivation of a quantitative path-wise descent-rate envelope over the entire descent is left for future work.

3.3 Convex formulation via lossless convexification

A squared-L2 thrust-effort cost is used to penalize control effort. From the dynamics and constraints above, the emergency-landing trajectory-generation problem is formulated as the following optimal control problem (P):

$$\begin{aligned}
(\mathrm{P}) \quad & \min_{x,u} \int_{t_0}^{t_f} \|u(t)\|^2\, dt \\
& \text{s.t. } \dot{p} = v, \quad \dot{v} = \tfrac{1}{m}u + g, \\
& \quad u_{\min} \le \|u\| \le u_{\max}, \quad \|H_c u\| \le \tan(\theta_{\max})\, e_3^\top u, \\
& \quad x(t) \in \mathcal{X}, \quad x(t_0) = x_0, \quad x(t_f) \in \mathcal{X}_f
\end{aligned} \tag{7}$$

where X is the set of convex state-path constraints described in Section 3.2 (the glide-slope corridor, the altitude box, and the no-ascent condition), and Xf is the terminal boundary condition. In this problem the non-convexity arises solely from the thrust-magnitude lower bound, which makes (P) a non-convex optimal control problem whose global solution is in general difficult to obtain directly.

To remove this non-convexity, the lossless convexification (LCvx) technique is applied [1]. Introducing a slack variable sigma(t), the non-convex thrust-magnitude constraint is relaxed as

$$\|u(t)\| \le \sigma(t), \qquad u_{\min} \le \sigma(t) \le u_{\max} \tag{8}$$

This relaxation transforms the original problem (P) into the following relaxed problem (P-bar):

$$\begin{aligned}
(\bar{\mathrm{P}}) \quad & \min_{x,u,\sigma} \int_{t_0}^{t_f} \sigma(t)^2\, dt \\
& \text{s.t. } \dot{p} = v, \quad \dot{v} = \tfrac{1}{m}u + g, \\
& \quad \|u\| \le \sigma, \quad u_{\min} \le \sigma \le u_{\max}, \quad \|H_c u\| \le \tan(\theta_{\max})\, e_3^\top u, \\
& \quad x(t) \in \mathcal{X}, \quad x(t_0) = x_0, \quad x(t_f) \in \mathcal{X}_f
\end{aligned} \tag{9}$$

The relaxed problem (P-bar) is a convex problem consisting only of second-order cone, box, and affine constraints, and transcribing the continuous-time dynamics on a uniform grid using the trapezoidal rule yields a finite-dimensional second-order cone program (SOCP). SOCPs are convex optimization problems for which globally optimal solutions can be obtained efficiently using standard solvers. This makes the formulation suitable for computationally efficient onboard trajectory generation, although real-time performance is not quantified in this paper. For a fixed phase duration the discretized relaxed problem is an SOCP, and the phase durations themselves are not optimized inside the SOCP but are determined through an outer feasibility-based time search (Section 3.4).

The relaxed solution is useful only if it also satisfies the original non-convex thrust constraint. In the LCvx formulation, the thrust-magnitude lower bound is replaced by the slack-variable constraints. Therefore, the relaxation is exact when the optimal solution satisfies the equality between the thrust magnitude and the slack

variable; in that case, the relaxed solution is feasible for the original problem. This property, by which the relaxed solution exactly recovers the solution of the original non-convex problem, is called the losslessness, or exactness, of the relaxation. LCvx theory shows that this equality is guaranteed if a sufficient thrust-margin condition holds, under which the thrust-magnitude lower bound is not active at the optimal solution. Since the present emergency-landing problem requires sufficient thrust to counteract gravity during descent, such a condition is expected to hold, and the exactness is confirmed numerically for the generated trajectory (Section 4). A rigorous certification of this condition is left for future work.

3.4 Two-phase coupling and time allocation

The convex trajectory-generation problem formulated above is solved with a two-phase structure consisting of a landing-approach phase and a terminal-descent phase. The two phases are connected at the terminal landing-phase junction defined in Section 2.3, where the terminal state of the landing-approach phase becomes the initial state of the terminal-descent phase. That is, the landing-approach phase is solved to determine the state at the junction, and then the terminal-descent phase is solved sequentially using this state as the initial condition. Each phase is solved as an SOCP of the relaxed-problem form (P-bar) of Section 3.3, with flight times T1 and T2, respectively.

Since emergency landing requires a prompt touchdown, the framework selects the time allocation that minimizes the total flight time T_total = T1 + T2 within the range that satisfies the safety constraints. The flight time of each phase is determined in a time-search loop outside the SOCP: candidates (T1, T2) are searched over a grid, and the feasibility of the inner SOCP is checked for each candidate. The minimum feasible time allocation among the tested grid candidates is then selected.

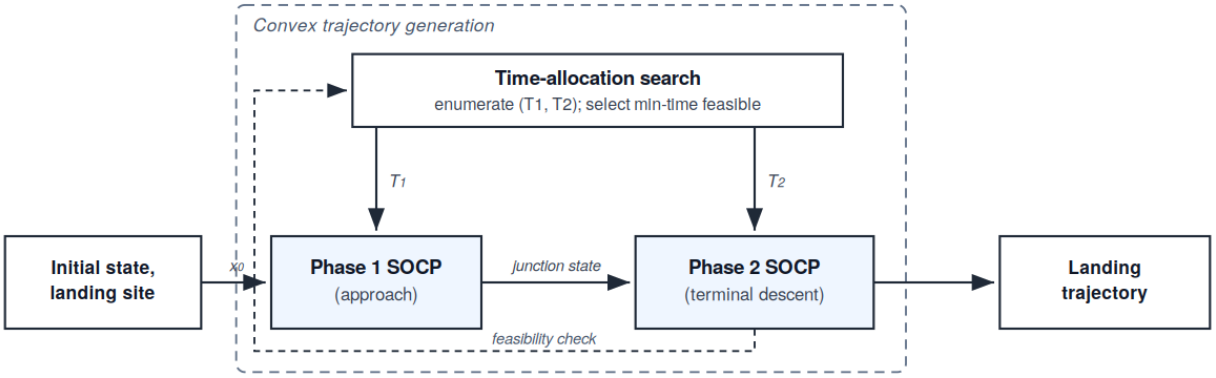


Figure 3 – Convex trajectory-generation framework with two-phase SOCP and the outer time-search loop.

4. Numerical Results

4.1 Simulation setup

This section presents a numerical simulation of the convex-optimization-based emergency-landing trajectory-generation framework. While the framework targets the full-scale OPPAV configuration described in Section 2.1, the numerical example uses the parameters of a scaled flight-test vehicle with the same propeller arrangement, with the main parameters given in Table 1. To illustrate the operation of the framework, a single emergency-landing scenario is considered. The aircraft starts at a position 300 m east, -30 m north, and 300 m in altitude relative to the landing site, with an initial velocity of (-3, 1, -2) m/s, and lands at the emergency landing site located at the origin. Each phase is discretized into 30 intervals (31 nodes), and the relaxed problem (P-bar) is solved using a standard SOCP solver.

Table 1. Vehicle and scenario parameters.

Parameter	Symbol	Value
Mass	m	5.0 kg
Vehicle diameter	D	1.2 m
Min. thrust	u_min	7.36 N (0.15 mg0)
Max. thrust	u_max	122.63 N (2.5 mg0)
Tilt limit (Phase 1 / 2)	theta_max	30 deg / 20 deg
Junction altitude	h_top	30.5 m
Glide-slope angle	gamma_glide	70 deg
Touchdown disk radius	R_td	1.5 m
Nodes per phase	N	31

4.2 Generated trajectory

Through the outer time search, T_total = 53.0 s (T_1 = 41.7 s, T_2 = 11.3 s) was selected as the minimum total flight time satisfying the safety constraints among the tested grid candidates. Figure 4 shows the resulting three-dimensional landing trajectory. The landing-approach and terminal-descent phases are connected continuously at the junction, and during terminal descent the trajectory remains inside the frustum corridor and approaches the touchdown disk at the landing site. Figure 5 and Figure 6 show the time histories of position and velocity, respectively. The aircraft transitions from the landing-approach phase to the terminal-descent phase at the junction altitude, and the velocity reaches zero at touchdown, satisfying a zero-velocity touchdown condition. In this numerical example, zero touchdown velocity is imposed as a terminal condition more conservative than the allowable landing-gear sink-rate limit.

4.3 Constraint satisfaction and relaxation exactness

Figure 7 shows the time history of the thrust magnitude. The thrust magnitude is maintained within the annular bounds over the entire interval, and the thrust-direction tilt constraint, the glide-slope corridor, and the altitude constraint are also satisfied at all nodes. To confirm the exactness of the relaxation described in Section 3.3, the relaxation gap and the thrust magnitude of the resulting solution were examined. At all discrete nodes, the relaxation gap was within the numerical tolerance (about 1e-8), and the recovered thrust magnitude satisfied the lower bound (minimum lower-bound margin 38.9 N). These results indicate that, for this scenario, the relaxed solution is feasible for the original non-convex thrust constraint and that the relaxation is exact within numerical tolerance.

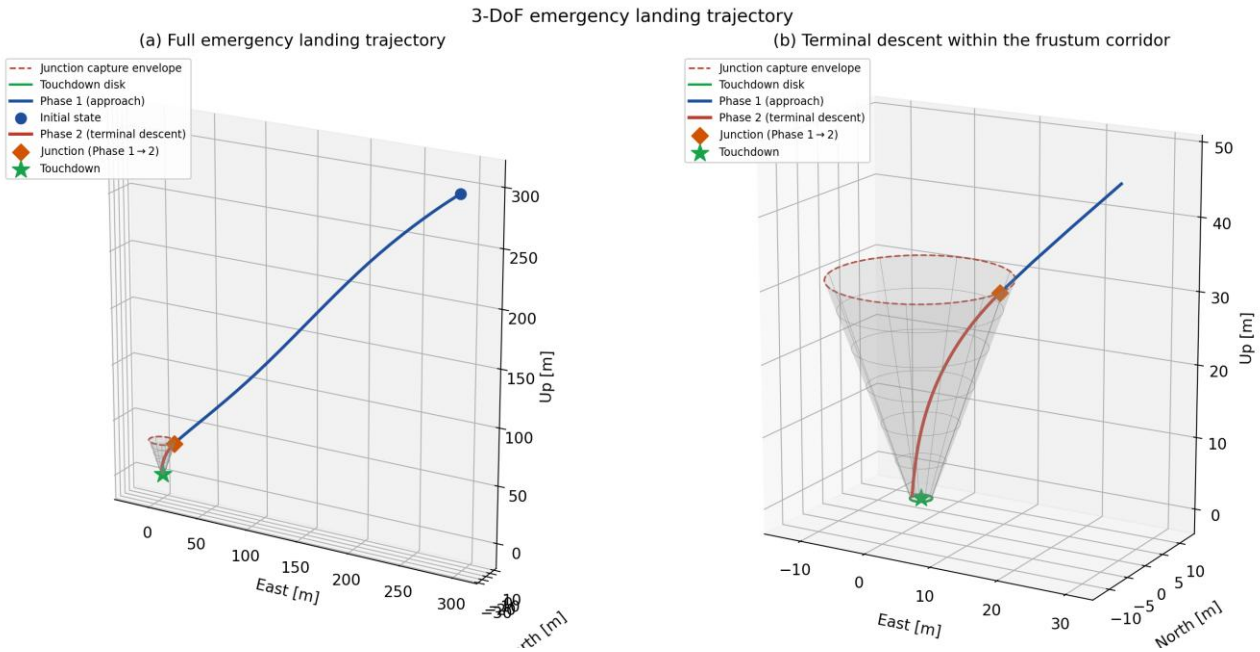


Figure 4 – Resulting three-dimensional emergency-landing trajectory.

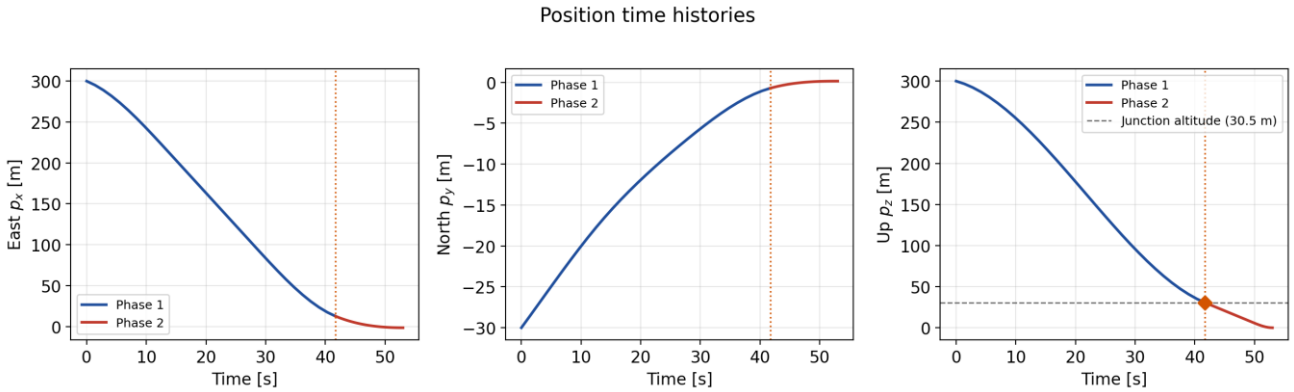


Figure 5 – Position time histories.

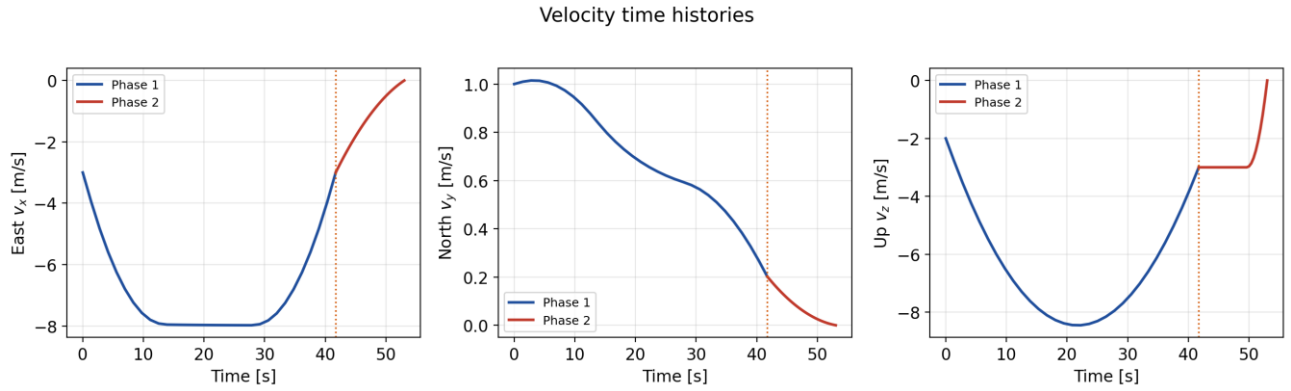


Figure 6 – Velocity time histories.

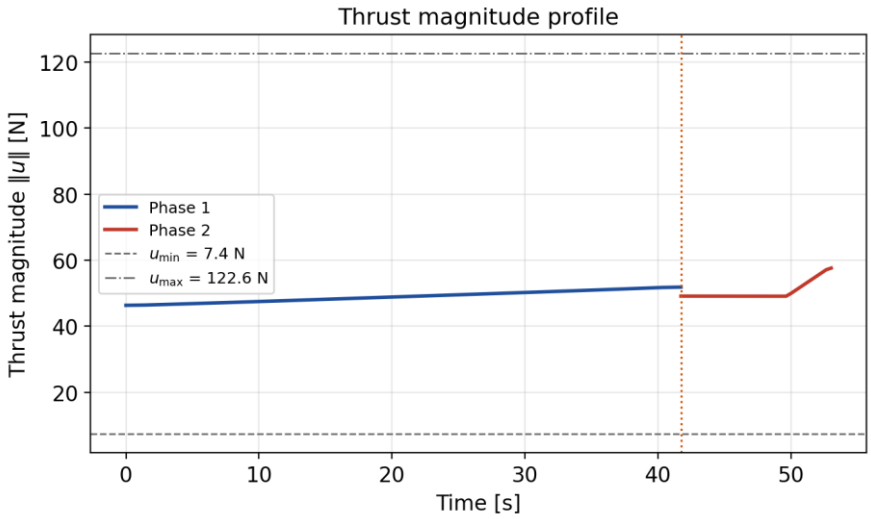


Figure 7 – Thrust-magnitude profile with the annular bounds.

5. Conclusion

This paper presented a regulation-informed convex trajectory-generation framework for eVTOL emergency landing. The framework combines a two-phase landing profile, defined using representative CEL requirements as design references, with an LCvx-based SOCP formulation of the thrust-constrained trajectory-generation problem. A numerical example demonstrated that the resulting trajectory satisfies the thrust and landing-geometry constraints. The relaxation gap and lower-thrust margin further showed that the relaxed solution is feasible for the original non-convex thrust constraint in the tested scenario.

Future work will focus on quantitative safe-descent criteria, a more rigorous exactness analysis, and extension

to 6-DoF flight dynamics. Flight-test validation, obstacle avoidance, and perception-based emergency-landing-site identification will also be addressed to support deployment in dense urban environments.

Contact Author Email Address

Corresponding author: jyd28@kari.re.kr

Copyright Statement

The authors confirm that they, and/or their company or organization, hold copyright on all of the original material included in this paper. The authors also confirm that they have obtained permission, from the copyright holder of any third party material included in this paper, to publish it as part of their paper. The authors confirm that they give permission, or have obtained permission from the copyright holder of this paper, for the publication and distribution of this paper as part of the ICAS proceedings or as individual off-prints from the proceedings.

References

[1] B. Açıkmeşe and L. Blackmore, “Lossless Convexification of a Class of Optimal Control Problems with Non-Convex Control Constraints,” Automatica, vol. 47, no. 2, pp. 341–347, 2011.

[2] D. P. Scharf, B. Açıkmeşe, D. Dueri, J. Benito, and J. Casoliva, “Implementation and Experimental Demonstration of Onboard Powered-Descent Guidance,” Journal of Guidance, Control, and Dynamics, vol. 40, no. 2, pp. 213–229, 2017.

[3] Z. Wang, P. Wei, and L. Sun, “Optimal Cruise, Descent, and Landing of eVTOL Vehicles for Urban Air Mobility Using Convex Optimization,” AIAA SciTech 2021 Forum, AIAA Paper 2021-0577, 2021.

[4] Y. Wu, S. Deniz, Y. Shi, and Z. Wang, “Convex Approach to Real-Time Multiphase Trajectory Optimization for Urban Air Mobility,” Journal of Air Transportation, vol. 33, no. 1, pp. 69–85, 2025.

[5] European Union Aviation Safety Agency, “Special Condition for Small-Category VTOL Aircraft,” Doc. No. SC-VTOL-01, Issue 1, 2 July 2019.

[6] European Union Aviation Safety Agency, “Second Publication of Means of Compliance with the Special Condition VTOL,” Doc. No. MOC-2 SC-VTOL, Issue 3, 22 December 2022.

[7] European Union Aviation Safety Agency, “Prototype Technical Specifications for the Design of VFR Vertiports (PTS-VPT-DSN),” March 2022.

[8] European Union Aviation Safety Agency, “Certification Specifications for Small Rotorcraft (CS-27),” Amendment 10, 2022.

[9] Federal Aviation Administration, “Airworthiness Criteria: Special Class Airworthiness Criteria for the Joby Aero, Inc. Model JAS4-1 Powered-Lift,” Federal Register, vol. 89, no. 47, pp. 17230–17264, 8 March 2024, Docket No. FAA-2021-0638.